Dicarba α-Conotoxin Vc1.1 Analogues with Differential Selectivity for Nicotinic Acetylcholine and GABA B Receptors

ARTICLE *in* ACS CHEMICAL BIOLOGY · JUNE 2013

Impact Factor: 5.33 · DOI: 10.1021/cb4002393 · Source: PubMed

10 AUTHORS, INCLUDING:

Bianca J Van Lierop
University of Ottawa
22 PUBLICATIONS **215** CITATIONS
SEE PROFILE

Shiva Nag Komeplla
RMIT University
14 PUBLICATIONS **76** CITATIONS
SEE PROFILE

Jeff Robert Mcarthur
Harvard University
17 PUBLICATIONS **281** CITATIONS
SEE PROFILE

Andrew Hung
RMIT University
39 PUBLICATIONS **748** CITATIONS
SEE PROFILE

ACS chemical biology

Articles

pubs.acs.org/acschemicalbiology

Dicarba α-Conotoxin Vc1.1 Analogues with Differential Selectivity for Nicotinic Acetylcholine and $GABA_B$ Receptors

Bianca J. van Lierop,[†,⊥] Samuel D. Robinson,[‡,⊥] Shiva N. Kompella,[§,⊥] Alessia Belgi,[†] Jeffrey R. McArthur,[§] Andrew Hung,[§] Christopher A. MacRaild,[‡] David J. Adams,[§] Raymond S. Norton,[‡] and Andrea J. Robinson*[,†]

[†]School of Chemistry, Monash University, Clayton 3800, Victoria, Australia

[‡]Medicinal Chemistry, Monash Institute of Pharmaceutical Sciences, Monash University, Parkville 3052, Victoria, Australia

[§]Health Innovations Research Institute, RMIT University, Bundoora 3083, Victoria, Australia

Supporting Information

ABSTRACT: Conotoxins have emerged as useful leads for the development of novel therapeutic analgesics. These peptides, isolated from marine molluscs of the genus *Conus*, have evolved exquisite selectivity for receptors and ion channels of excitable tissue. One such peptide, α-conotoxin Vc1.1, is a 16-mer possessing an interlocked disulfide framework. Despite its emergence as a potent analgesic lead, the molecular target and mechanism of action of Vc1.1 have not been elucidated to date. In this paper we describe the regioselective synthesis of dicarba analogues of Vc1.1 using olefin metathesis. The ability of these peptides to inhibit acetylcholine-evoked current at rat α9α10 and α3β4 nicotinic acetylcholine receptors (nAChR) expressed in *Xenopus* oocytes has been assessed in addition to their ability to inhibit high voltage-activated (HVA) calcium channel current in isolated rat DRG neurons. Their solution structures were determined by NMR spectroscopy. Significantly, we have found that regioselective replacement of the native cystine framework with a dicarba bridge can be used to selectively tune the cyclic peptide's innate biological activity for one receptor over another. The 2,8-dicarba Vc1.1 isomer retains activity at γ-aminobutyric acid ($GABA_B$) G protein-coupled receptors, whereas the isomeric 3,16-dicarba Vc1.1 peptide retains activity at the α9α10 nAChR subtype. These singularly acting analogues will enable the elucidation of the biological target responsible for the peptide's potent analgesic activity.

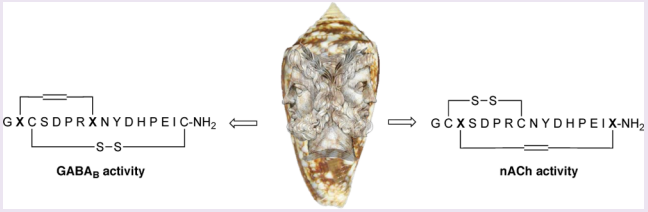

α-Conotoxin Vc1.1 is a cysteine-rich peptide isolated from the venom of *Conus victoriae*, a predatory cone snail found in Australian waters.[1−3] It is an antagonist of the α9α10 subtype of nicotinic acetylcholine receptors (nAChRs)[4] and a potent antagonist of N-type calcium channel function, *via* agonism of the γ-aminobutyric acid ($GABA_B$) G protein-coupled receptor.[5−9] Although the molecular target and mechanism of action of Vc1.1 for the treatment of neuropathic pain are not yet clear,[10,11] the therapeutic potential of this peptide is well established.[12] In this study, carbon-based analogues of the disulfide-stabilized conotoxin Vc1.1 have been synthesized in order to probe the preferred S−S torsional and dihedral angles within the bioactive peptide. The dicarba mimetics described herein possess defined hybridization and stereochemistry and therefore provide an elegant way to probe the structural and functional roles of the native disulfide bridges and the optimum conformation for receptor interaction.

RESULTS AND DISCUSSION

The synthesis of four globular unsaturated dicarba-cystino Vc1.1 peptide analogues was achieved by microwave-assisted ring-closing metathesis of L-allylglycine residues. The precursor linear peptides were prepared by Fmoc solid-phase peptide synthesis on rink amide resin to yield C-terminally amidated peptides (Supplementary Figure 1). The metathesis-active residues were incorporated in positions 2 and 8 to generate the loop I dicarba analogues (A and B) and in positions 3 and 16 to yield the loop II dicarba analogues (C and D, Figure 1). On-resin ring-closing metathesis proceeded quantitatively after 1−2 h of continuous microwave irradiation in the presence of 20 mol % second-generation Grubbs catalyst. Following formation of the unsaturated dicarba bridge, the peptides were cleaved from the resin, and buffered aerial oxidation of the cysteine residues resulted in the formation of the cystine bridge. The crude peptides were then purified by RP-HPLC, analyzed spectroscopically, and subjected to biological testing (Supplementary Figure 2).

Regioselective installation of the dicarba bridge is defined by the primary sequence. We have previously shown that in many peptides the native disulfide bridge can be replaced with the dicarba mimetic without loss of function.[13−16] The tertiary structure of α-conotoxins is highly conserved, with the side

Received: April 7, 2013
Accepted: June 2, 2013
Published: June 2, 2013

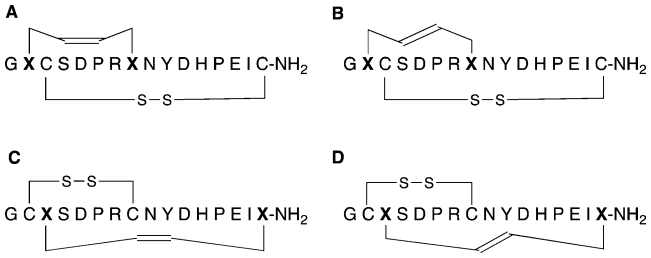

Figure 1. Four unsaturated dicarba-cystino Vc1.1 α-conotoxin analogues: Loop I analogues, *cis*-[2,8]-dicarba Vc1.1 (A) and *trans*-[2,8]-dicarba Vc1.1 (B); Loop II analogues, *cis*-[3,16]-dicarba Vc1.1 (C) and *trans*-[3,16]-dicarba Vc1.1 (D). X shows the positional sequence insertion of L-allylglycine residues prior to ring-closing olefin metathesis cyclization.

chains making key interactions with receptors to elicit activity. Here we have used NMR spectroscopy to examine the effects of the dicarba substitutions on the Vc1.1 structure across the four isomers (A–D).

A summary of experimental NMR constraints and structural statistics for the dicarba Vc1.1 analogues is given in Supplementary Table 5. All structures were well-defined across most of their sequence (φ and ψ angular order parameters >0.8), with the exception of the C-terminus (residues 13–15) of *trans*-[2,8]-dicarba Vc1.1. This peptide lacked the His12 H^{β}–Ile15 $H^{\beta/\gamma/\delta}$ NOEs and His12 $H^{\alpha/\beta}$–14Glu H^{N} NOEs present in the other two isomers, indicating a different loop II conformation. As the chemical shifts for the *cis* and *trans* isomers of [3,16]-dicarba Vc1.1 were essentially identical (Supplementary Figure 6), structures are shown below for the *trans*-[3,16] isomer only.

The closest-to-average structures of *cis*-[2,8]-dicarba Vc1.1 and *trans*-[3,16]-dicarba Vc1.1 (Figure 2) are both characterized by an α-helix spanning residues 6–11 (as in native Vc1.1). Medium-range NOEs in this region support the presence of helical structure in both peptides. The *N*-terminal region (residues 2–4) also forms a 3_{10}-helix in 11 and 18 of the 20 final structures of *cis*-[2,8]-dicarba Vc1.1 and *trans*-[3,16]-dicarba Vc1.1, respectively. In contrast, the closest-to-average structure of *trans*-[2,8]-dicarba Vc1.1 (Figure 2D) contains no helical structure; indeed, a more extended structure for this peptide is supported by a lack of medium-range NOEs in this region and dihedral angles characteristic of a β-turn for residues Asn9 and Tyr10. In all of the final structures of the analogues a β-turn occurs at Asp5, another structural feature seen in native Vc1.1.

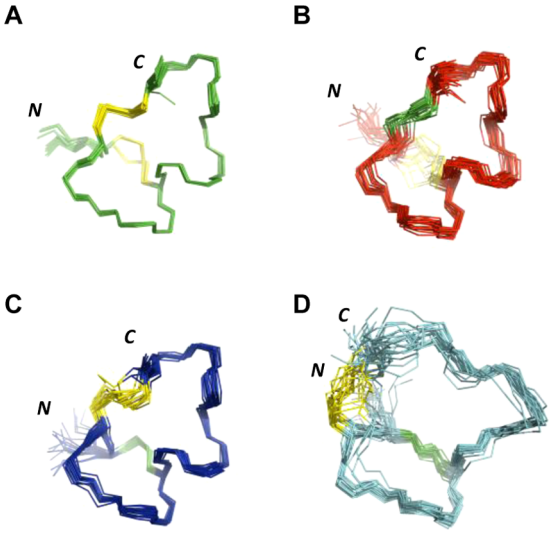

Figure 2. Ensemble of 20 structures of Vc1.1 (PDB ID 2H8S) (A) compared with those of *trans*-[3,16]- (B), *cis*-[2,8]- (C), and *trans*-[2,8]-dicarba Vc1.1 (D). Disulfide bonds are shown in yellow, dicarba bonds are in green, and N- and C-termini are labeled.

The backbone conformations of *cis*-[2,8]-dicarba Vc1.1 and *trans*-[3,16]-dicarba Vc1.1 (Figure 3) are essentially identical to

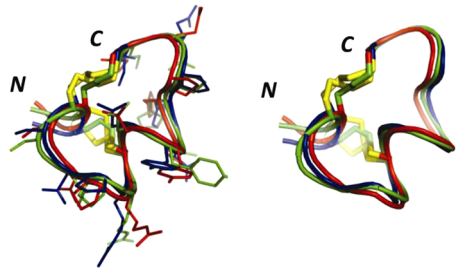

Figure 3. Closest-to-average structures of Vc1.1 (PDB ID 2H8S) (green) overlaid with those of *trans*-[3,16]- (red) and *cis*-[2,8]-dicarba Vc1.1 (blue). The dicarba bridges are shown in green, disulfide bridges are in yellow, and N- and C-termini are labeled.

that of the native structure (backbone heavy atomic RMSD 0.27 Å (residues 4–16) and 0.36 Å (residues 5–16), respectively). However, the backbone conformation of *trans*-[2,8]-dicarba Vc1.1 (Figure 2D) is very different from those of both of these analogues and native Vc1.1. The most notable perturbation is seen through loop II of the peptide (residues 10–15) and the loss of helical structure following residue 9. The *N*-terminal region (residues 1–3) is also affected. Loop I (residues 4–7), however, appears to retain a structure very similar to those of the other analogues and of native Vc1.1 (backbone heavy atomic RMSD 0.40 Å over residues 4–9).

The dicarba Vc1.1 analogues described here possess remarkable selectivity at both of their biological targets. In this study, each of the peptides was compared with native Vc1.1 on $\alpha9\alpha10$ and $\alpha3\beta4$ nAChRs expressed in *Xenopus* oocytes and on high voltage-activated (HVA) calcium channels in rat dorsal root ganglion (DRG) neurons. Native Vc1.1 reversibly inhibited ACh-evoked $\alpha9\alpha10$ nAChR-mediated currents in a concentration-dependent manner with an IC_{50} of 75.0 ± 1.0 nM and a Hill coefficient of 1.4 ± 0.2 (n = 4), consistent with previously reported data.[10] The *cis*- and *trans*-[3,16]-dicarba Vc1.1 analogues displayed differing abilities to inhibit ACh-evoked currents: the *trans* isomer exhibited an IC_{50} of 2.4 ± 0.3 μM and a Hill coefficient of 1.5 ± 0.3 (n = 4), and the *cis* isomer was ~5-fold less active with an IC_{50} of 12.0 ± 3.0 μM and a Hill coefficient of 0.8 ± 0.2 (n = 4) (Figure 4A and C). A similar trend was observed for these peptides at the $\alpha3\beta4$ nAChR subtype (Figure 4B). Significantly, replacement of the [2,8]-cystine bridge had a profound effect on nAChR activity, with both the *cis*- and *trans*-[2,8]-dicarba Vc1.1 peptides being devoid of activity at the $\alpha9\alpha10$ receptor (Figure 4C).

We also examined the inhibition of HVA calcium channel currents in rat DRG neurons. Inhibition by native Vc1.1 is known to be concentration-dependent with an IC_{50} value of 1.7 nM.[5] It has been shown previously that HVA calcium channel current inhibition by Vc1.1 and its analogues is due to G protein-coupled $GABA_B$ receptor-mediated inhibition of N-type

dx.doi.org/10.1021/cb4002393 | ACS Chem. Biol. 2013, 8, 1815–1821

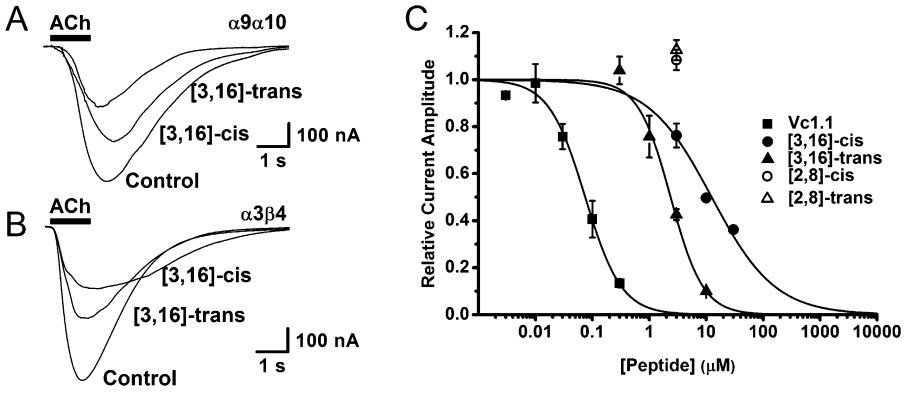

Figure 4. Inhibition of ACh-evoked currents by dicarba α-conotoxin Vc1.1 analogues at rat $\alpha9\alpha10$ and $\alpha3\beta4$ nAChRs expressed in *Xenopus* oocytes. (A) Superimposed ACh (50 μM)-evoked currents mediated by $\alpha9\alpha10$ nAChRs in the absence (Control) and presence of 3 μM *trans*-[3,16]-dicarba Vc1.1 and *cis*-[3,16]-dicarba Vc1.1. (B) Superimposed ACh (50 μM)-evoked currents at $\alpha3\beta4$ nAChRs in the absence (Control) and presence of 30 μM *trans*-[3,16]-dicarba Vc1.1 and *cis*-[3,16]-dicarba Vc1.1. (C) Concentration−response curves obtained for all peptides examined at $\alpha9\alpha10$ nAChRs ($n \geq 4$ for each peptide). *trans*-[2,8]-Dicarba Vc1.1 and *cis*-[2,8]-dicarba Vc1.1 (3−10 μM) were inactive at $\alpha9\alpha10$ nAChRs.

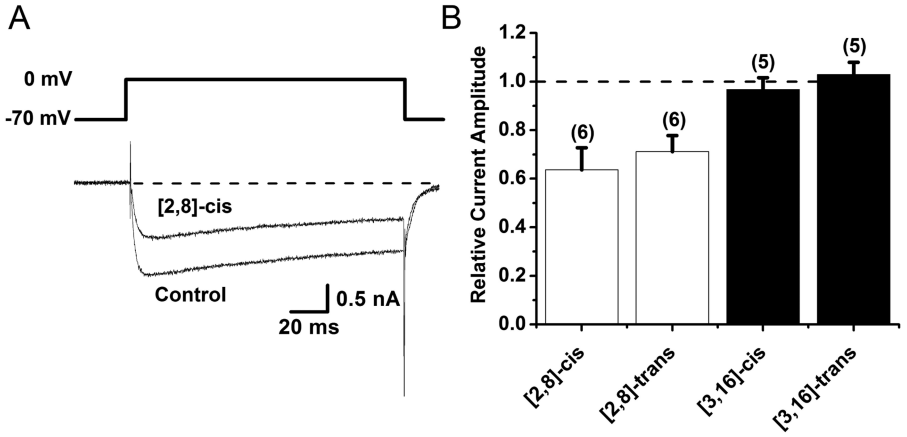

Figure 5. Inhibition of high voltage-activated (HVA) calcium channel currents in isolated rat DRG neurons by dicarba α-conotoxin Vc1.1 analogues. (A) Superimposed depolarization-activated whole-cell Ba^{2+} currents elicited by a 150 ms voltage step to 0 mV from a holding potential of −70 mV in the absence (Control) and presence of 100 nM *cis*-[2,8]-dicarba Vc1.1. (B) Bar graph of relative inhibition of HVA calcium channel currents by 100 nM *cis*-[2,8]-dicarba Vc1.1 (n = 6), 100 nM *trans*-[2,8]-dicarba Vc1.1 (n = 6), 1 μM *cis*-[3,16]-dicarba Vc1.1 (n = 5), and 1 μM *trans*-[3,16]-dicarba Vc1.1 (n = 5).

($Ca_v2.2$) calcium channels in DRG neurons.[5−9] The relative potencies of the four dicarba Vc1.1 analogues were again found to differ in their ability to inhibit HVA Ca^{2+} channel currents. Remarkably, the [3,16]-dicarba analogues, which were active against nAChR, were now inactive at the $GABA_B$ receptor-modulated N-type calcium channel in DRG neurons. In stark contrast, the nAChR-inactive [2,8]-dicarba analogues were found to act via $GABA_B$ receptors and potently inhibit HVA Ca^{2+} channel current (Figures 5A and B). The inhibition of HVA Ca^{2+} channel currents by the [2,8]-dicarba Vc1.1 analogues was antagonized in the presence of 1 μM CGP 55845, a selective $GABA_B$ receptor antagonist (data not shown).

While the loss in activity at the nAChR of the *trans*-[2,8]-dicarba Vc1.1 analogue might be explained by the clear perturbation of its three-dimensional structure, the change observed in the *cis*-[2,8]-dicarba Vc1.1 was more subtle. Additionally, any structural change observed in *trans*-[3,16]-dicarba Vc1.1 can only be described as minor, but dramatic effects on the peptide's pharmacological profile are observed. As the latter two peptides have similar structures yet significant differences in activity, the remainder of the discussion will focus primarily on them.

In Vc1.1, point mutation studies have implicated two distinct regions of the peptide, namely, residues Asp5-Arg7 in loop I and Asp11-Ile15 in loop II, as critical for the pharmacological activity of the peptide.[17] Each of these regions is presumably finely tuned in space in relation to one another, and they act in concert to determine the pharmacological properties of the peptide. We propose that the cystine residues of Vc1.1 also contribute to its activity on the basis that substitution of the Cys2-8 disulfide results in loss of activity at nAChRs, while substitution of the Cys3-16 disulfide results in loss of activity at the $GABA_BR$, most importantly, without any dramatic changes in the three-dimensional structure of the peptides.

The α-conotoxin variant PnIA[A4L,D14K] is a 16-residue peptide with a 4/7 loop pattern and an identical *N*-terminal sequence (GCCS) to Vc1.1. The crystal structure of PnIA-[A4L,D14K] bound to the AChBP (a homologue of the nAChR ligand binding domain) has shown that Gly1, Cys2, and Ser4 interact with the receptor.[18,19] Interestingly, the Cys2-8 disulfide bond is stacked on the vicinal Cys188-189 disulfide on the principal face of the AChBP binding site. It is likely that

dx.doi.org/10.1021/cb4002393 | *ACS Chem. Biol.* 2013, 8, 1815−1821

this is also the case for Vc1.1 bound to $\alpha9\alpha10$. With this in mind we propose a possible scenario to explain the loss in activity of our [2,8]-dicarba Vc1.1 analogues at the nAChR, in which the Cys2-8 disulfide bond, when replaced by a dicarba bridge, can no longer form the natural stacking interaction with the disulfide of the C-loop. This scenario explains why all three peptides can share a similar three-dimensional structure yet differ so remarkably in activity. It also implicates the 3,16-disulfide bond of Vc1.1 as important for $GABA_BR$ activity. To model the functional consequences of the scenario described above, the ligand binding domain of $\alpha9\alpha10$ complexed with wild-type Vc1.1 or *cis*-[2,8]- or *trans*-[3,16]-dicarba Vc1.1 was studied in solvated molecular dynamics (MD) simulations (Figure 6). At both $\alpha9(+)\alpha10(-)$ and $\alpha10(+)\alpha9(-)$ interfaces,

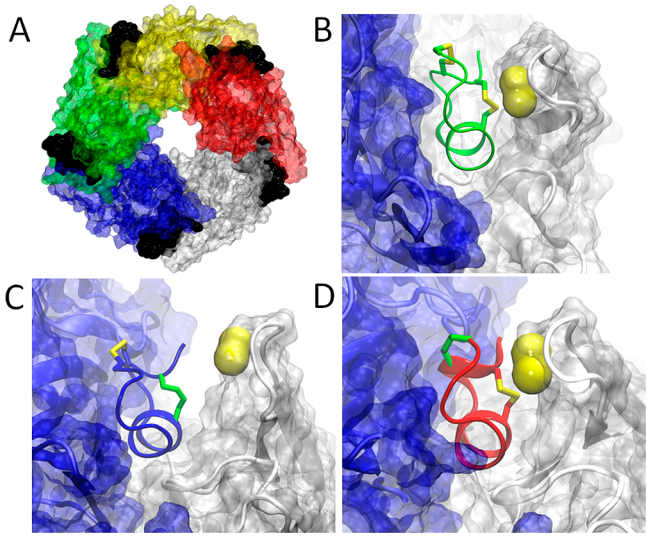

Figure 6. Surface representation of the $\alpha9\alpha10$ homology model based on AChBP bound to the α-conotoxin variant PnIA (A4L, D14K) (PDB ID 2BR8), with Vc1.1 shown in black (A). MD simulation snapshot at 100 ns of native Vc1.1 (green) (B), *cis*-[2,8]-dicarba Vc1.1 (blue) (C), and *trans*-[3,16]-dicarba Vc1.1 (red) (D) bound at the $\alpha9(+)\alpha10(-)$ interface. The dicarba bridge is shown in green, and disulfide bridges are in yellow. Receptor $\alpha9(+)$ is shown in white, and $\alpha10(-)$ is in blue. The vicinal $\alpha9(+)$ disulfide is highlighted yellow.

simulations indicate loss of contacts between the *cis*-[2,8]-dicarba alkene carbons with key residues at the tip of the C-loop of the principal face (Figure 6C) relative to native Vc1.1 (Figure 6B). This arises due to the inability of dicarba alkene carbons to form effective stacking interactions with the receptor disulfides and "aromatic cage" residues such as Y216. At the $\alpha10(+)\alpha9(-)$ face, simulations also indicate a reduction in contacts between the toxin and amphiphilic residues at the complementary face. Loss of contacts between the toxin dicarba alkenes and key receptor binding site residues, relative to native Vc1.1, may partly explain the reduced potency of the *cis*-[2,8]-dicarba analogue at the nAChR.

Structurally, conotoxins are best described as small rigid scaffolds that display amino acids on their surface to selectively target their receptors. Vc1.1 is a finely tuned structure with several distinct regions that combine to produce its unique pharmacological activity profile. Our results suggest that the disulfide bonds in conotoxins are critical for the structure of the peptide, as well as contributing directly to receptor binding. In conclusion, not only are our dicarba analogues valuable as probes of the structure−activity relationships of Vc1.1 against its different targets, but they also provide more stable lead compounds for future antinociceptive testing.

METHODS

Peptide Synthesis and Characterization. *[2,8]-Agl-[3,16]-Cys Conotoxin Vc1.1.* Synthesis of the linear sequence was performed according to the microwave-accelerated SPPS procedure described in the Supporting Information using rink amide resin (250 mg, 100 μmol). RP-HPLC and mass spectral analysis of an aliquot of Fmoc- and resin-cleaved peptide supported formation of the required linear sequence in 85% purity. Mass spectrum (ESI^+, $MeCN/H_2O/HCOOH$): m/z 600.4 $[M + 3H]^{3+}$, $1/3(C_{75}H_{114}N_{23}O_{25}S_2)$ requires 600.3; 900.0 $[M + 2H]^{2+}$, $1/2(C_{75}H_{113}N_{23}O_{25}S_2)$ requires 899.9. RP-HPLC (Agilent, Vydac C18 analytical column, 10% → 30% buffer B over 30 min): t_R = 16.6 min.

c[$\Delta^4$2,8]-Dicarba-[3,16]-Cys Conotoxin Vc1.1. Resin-bound peptide was subjected to the microwave-accelerated RCM procedure described above under the following conditions: resin-bound linear peptide (575 mg, 100 μmol), DCM (4.75 mL), 0.4 M LiCl in DMF (0.25 mL), second generation Grubbs catalyst (17 mg, 20 μmol), 100 W μwave, 100 °C, 1 h, 100% conversion into the target peptide. RP-HPLC and mass spectral analysis of an aliquot of Fmoc- and resin-cleaved peptide supported formation of the required unsaturated carbocycle in 85% purity. Mass spectrum (ESI^+, $MeCN/H_2O/HCOOH$): m/z 591.2 $[M + 3H]^{3+}$, $1/3(C_{73}H_{110}N_{23}O_{25}S_2)$ requires 590.9; 886.0 $[M + 2H]^{2+}$, $1/2(C_{73}H_{109}N_{23}O_{25}S_2)$ requires 885.9. RP-HPLC (Agilent, Vydac C18 analytical column, 10% → 30% buffer B over 30 min): t_R = 14.3 min (broad). The remaining resin-bound peptide was then subjected to Fmoc-deprotection and acid-mediated cleavage to give a pale brown solid (118 mg).

c[$\Delta^4$2,8]-Dicarba-c[3,16]-cystino Conotoxin Vc1.1. The disulfide oxidation of the unsaturated ring-closed peptide was carried out according to a procedure described by Clark et al.[7] The monocyclic peptide (118 mg, 66.6 μmol) in H_2O/MeCN (10 mL; 1:1) was added to a stirred solution of 0.1 M NH_4HCO_3 (444 mL) at RT under a constant stream of air. Reaction progress was monitored by RP-HPLC (Agilent, Vydac C18 analytical column, 10% → 30% buffer B over 30 min, t_R = 13.3) and mass spectrometry. After 24 h, the reaction mixture was acidified to pH 2 with glacial AcOH and purified by preparative RP-HPLC (buffer A = 20 mM aqueous triethylammonium acetate. Buffer B = buffer A/MeCN (1: 9), Agilent, Vydac C18 preparative column, 10% → 20% buffer B over 30 min, t_R = 15.4 and 17.6 min) using a neutral buffer system in order to separate the geometric isomers (7: 3 ratio). Selected fractions were combined and lyophilized to give two isomers of peptide as colorless oils in >99% purity. *cis*-[2,8]-Dicarba Vc1.1: RP-HPLC (Agilent, Vydac C18 analytical column, 10% → 20% buffer B over 30 min): t_R = 14.2 min. *trans*-[2,8]-Dicarba Vc1.1: RP-HPLC (Agilent, Vydac C18 analytical column, 10% → 20% buffer B over 30 min): t_R = 17.5 min. Separate repurification of each bicyclic peptide *cis*-[2,8]-dicarba Vc1.1 and *trans*-[2,8]-dicarba Vc1.1 was then performed by RP-HPLC (Agilent, Vydac C18 preparative column, 10% → 30% buffer B over 30 min, t_R = 15.4 and 15.4 min) using an acidic buffer system to give each isomer of peptide as a colorless solid (*cis*-[2,8]-dicarba Vc1.1, 21.5 mg, 24% and *trans*-[2,8]-dicarba Vc1.1, 2.7 mg, 3%) in >99% purity. *cis*-[2,8]-Dicarba Vc1.1: mass spectrum (ESI^+, $MeCN/H_2O/HCOOH$): m/z 590.3 $[M + 3H]^{3+}$, $1/3(C_{73}H_{108}N_{23}O_{25}S_2)$ requires 590.2; 884.8 $[M + 2H]^{2+}$, $1/2(C_{73}H_{107}N_{23}O_{25}S_2)$ requires 884.9. RP-HPLC (Agilent, Vydac C18 analytical column, 10% → 30% buffer B over 30 min): t_R = 13.5 min. *trans*-[2,8]-Dicarba Vc1.1: mass spectrum (ESI^+, $MeCN/H_2O/HCOOH$): m/z 590.2 $[M + 3H]^{3+}$, $1/3(C_{73}H_{108}N_{23}O_{25}S_2)$ requires 590.2; 884.9 $[M + 2H]^{2+}$, $1/2(C_{73}H_{107}N_{23}O_{25}S_2)$ requires 884.9. RP-HPLC (Agilent, Vydac C18 analytical column, 10% → 30% buffer B over 30 min): t_R = 13.4 min.

[2,8]-Cys-[3,16]-Agl Conotoxin Vc1.1. Synthesis of the linear sequence was performed according to the microwave-accelerated SPPS procedure described in the Supporting Information using rink amide resin (250 mg, 100 μmol). RP-HPLC and mass spectral analysis of an aliquot of Fmoc- and resin-cleaved peptide supported formation

dx.doi.org/10.1021/cb4002393 | *ACS Chem. Biol.* 2013, 8, 1815−1821

of the required linear sequence in 75% purity. Mass spectrum (ESI^+, $MeCN/H_2O/HCOOH$): m/z 600.4 $[M + 3H]^{3+}$, 1/2($C_{75}H_{114}N_{23}O_{25}S_2$) requires 600.3; 900.0 $[M + 2H]^{2+}$, 1/2($C_{75}H_{113}N_{23}O_{25}S_2$) requires 899.9. RP-HPLC (Agilent, Vydac C18 analytical column, 10% → 30% buffer B over 30 min): t_R = 15.1 min.

[2,8]-Cys-c[Δ⁴3,16]-dicarba Conotoxin Vc1.1. Resin-bound peptide was subjected to the microwave-accelerated RCM procedure described above under the following conditions: resin-bound linear peptide (616 mg, 100 μmol), DCM (4.75 mL), 0.4 M LiCl in DMF (0.25 mL), second generation Grubbs catalyst (17 mg, 20 μmol), 100 W μwave, 100 °C, 2 h, 100% conversion into the required unsaturated carbocycle. RP-HPLC and mass spectral analysis of an aliquot of Fmoc- and resin-cleaved peptide supported formation of the required unsaturated carbocycle as two isomers, *trans*-[3,16]-dicarba Vc1.1 and *cis*-[3,16]-dicarba Vc1.1, in a 6:4 ratio. *trans*-[3,16]-Dicarba Vc1.1: mass spectrum (ESI^+, $MeCN/H_2O/HCOOH$): m/z 591.0 $[M + 3H]^{3+}$, 1/2($C_{73}H_{110}N_{23}O_{25}S_2$) requires 590.9; 886.0 $[M + 2H]^{2+}$, 1/2($C_{73}H_{109}N_{23}O_{25}S_2$) requires 885.9. RP-HPLC (Agilent, Vydac C18 analytical column, 10% → 30% buffer B over 30 min): t_R = 11.7 min. *cis*-[3,16]-Dicarba Vc1.1: mass spectrum (ESI^+, $MeCN/H_2O/HCOOH$): m/z 591.0 $[M + 3H]^{3+}$, 1/2($C_{73}H_{110}N_{23}O_{25}S_2$) requires 590.9; 886.0 $[M + 2H]^{2+}$, 1/2($C_{73}H_{109}N_{23}O_{25}S_2$) requires 885.9. RP-HPLC (Agilent, Vydac C18 analytical column, 10% → 30% buffer B over 30 min): t_R = 12.3 min. The remaining resin-bound peptide was then subjected to Fmoc-deprotection and acid-mediated cleavage to give a pale brown solid (150 mg).

c[2,8]-Cystino-c[Δ⁴3,16]-dicarba Conotoxin Vc1.1. The disulfide oxidation of the unsaturated ring-closed peptide was carried out according to a procedure described by Clark et al.[7] The monocyclic peptide (150 mg, 85 μmol) in H_2O/MeCN (10 mL; 1:1) was added to a stirred solution of 0.1 M NH_4HCO_3 (567 mL) at RT under a constant stream of air. Reaction progress was monitored by RP-HPLC (Agilent, Vydac C18 preparative column, 10% → 30% buffer B over 30 min) and mass spectrometry. After 18 h the reaction mixture was acidified to pH 2 with glacial AcOH and purified by preparative RP-HPLC (Agilent, Vydac C18 preparative column, 10% → 20% buffer B over 60 min, t_R = 24.8 and 26.9 min). Selected fractions were combined and lyophilized to give two isomers of the desired peptide as colorless solids (*trans*-[3,16]-dicarba Vc1.1: 3.2 mg, 2% and *cis*-[3,16]-dicarba Vc1.1: 2.0 mg, 1%) in >99% and 97% purity, respectively. *trans*-[3,16]-Dicarba Vc1.1: mass spectrum (ESI^+, $MeCN/H_2O/HCOOH$): m/z 884.9 $[M + 2H]^{2+}$, 1/2($C_{73}H_{107}N_{23}O_{25}S_2$) requires 884.9. RP-HPLC (Waters, Vydac C18 analytical column, 10% → 20% buffer B over 30 min): t_R = 16.2 min. *cis*-[3,16]-Dicarba Vc1.1: mass spectrum (ESI^+, $MeCN/H_2O/HCOOH$): m/z 885.0 $[M + 2H]^{2+}$, 1/2($C_{73}H_{107}N_{23}O_{25}S_2$) requires 884.9. RP-HPLC (Waters, Vydac C18 analytical column, 10% → 20% buffer B over 30 min): t_R = 17.4 min.

NMR Spectroscopy. *Spectroscopy.* The samples were prepared by dissolving the freeze-dried peptide in 90% H_2O/10% ^2H_2O, pH 4.8 to a concentration of ∼500 μM (∼800 μM for *trans*-[3,16] dicarba Vc1.1). A series of one-dimensional ^1H spectra and two-dimensional homonuclear TOCSY spectra (spin lock time 80 ms) were acquired at 10, 15, 20, and 25 °C (and 30 °C for *trans*-[2,8]-dicarba Vc1.1) on a Varian Inova 600 MHz instrument. DQF-COSY spectra and NOESY spectra (mixing times 75, 150, and 250 ms) were acquired at 20 °C, at pH 3.3 and pH 4.8 on a Varian Inova 600 MHz instrument and Bruker Avance3 600 MHz instrument, respectively. Chemical shift assignments for backbone and side chain protons of both isomers were made by conventional analysis of two-dimensional TOCSY, DQF-COSY, and NOESY spectra (mixing time of 250 ms) acquired at 20 °C, at pH 3.3 and pH 4.8. ^{15}N chemical shifts were obtained from a ^{15}N-SOFAST-HMQC spectrum (pH 4.8, 20 °C) acquired on a Varian Inova 600 MHz instrument. ^{13}C chemical shifts were obtained from a ^{13}C-HSQC spectrum acquired in 100% ^2H_2O (20 °C and pH 5.3 (pH 4.8 for *trans*-[3,16] dicarba Vc1.1)) acquired on a Bruker Avance2 500 MHz spectrometer. Dioxane (chemical shift of 3.75) was used as a ^1H chemical shift reference; ^{13}C and ^{15}N chemical shifts were referenced indirectly.[20] All spectra were processed in TOPSPIN (version 3.0, Bruker Biospin) and were analyzed using CcpNmr-Analysis (version 2.1.5).

$^3J_{HN\text{-}H\alpha}$ coupling constants were measured from one-dimensional ^1H spectra or DQF-COSY spectra (pH 4.8, 20 °C). Coupling constants were converted to φ angle constraints on the following basis: $^3J_{HN\text{-}H\alpha}$ > 8 Hz, $\varphi = -120 \pm 40°$ and $^3J_{HN\text{-}H\alpha}$ < 6 Hz, $\varphi = -60 \pm 30°$. Additional dihedral angle constraints were generated in TALOS+.[21] Two-dimensional NOESY with mixing times of 75 and 250 ms and DQF-COSY spectra (pH 4.8, 20 °C) were analyzed to obtain χ^1 angle constraints and facilitate the stereospecific assignment of H^β protons. Amide temperature coefficient values were calculated for residues of each analogue by examination of one-dimensional spectra and two-dimensional TOCSY spectra acquired at a temperature range of 10−25 °C at 5 °C intervals.

Structure Calculations. Initial structures were generated using CYANA software (version 3.0)[22] and assessed in MOLMOL (version 2K.1).[23] NOESY spectra (250 ms mixing time) in 90% H_2O/10% ^2H_2O (pH 4.8, 20 °C) were used to generate distance constraints. The dicarba bridge was modeled as two Aba residues with the inter-residue distance constraints C^γ−C^γ, H−C^γ, and C^β−C^γ applied across the dicarba bridge. Structures were optimized for a low target function, and initial structures were used to resolve the assignment of several ambiguous NOEs. Once optimized in CYANA, the final constraint set was entered into XPLOR-NIH.[24] In XPLOR calculations, the C^γ−C^γ double bond was modeled explicitly, as described previously.[14] With conventional simulated annealing protocols, the restraint set was used to generate a new ensemble of 100 structures. Of the 100 structures generated, 50 were selected for further refinement by restrained energy minimization in water.[25] The 20 lowest energy structures generated were chosen for analysis. PROCHECK-NMR[25] was used for the validation of final structure calculations. Molecular representations were prepared using PyMOL (Delano, W.L. The PyMOL Molecular Graphics System (2002) Delano Scientific, San Carlos, CA, USA (http://www.pymol.org).

Electrophysiological Recordings from Exogenously Expressed nAChRs in *Xenopus* Oocytes. RNA preparation, oocyte preparation, and expression of nAChR subunits in *Xenopus* oocytes were performed as described previously.[17] Briefly, plasmids with cDNA encoding the rat α3, α9, α10, and β4 subunits subcloned into the oocyte expression vector pNKS2 were used for mRNA preparation using mMESSAGE mMACHINE Kit (Ambion; Life Technologies, Carlsbad, CA). Oocytes were injected with 10 ng of mRNA for α3 and β4 subunits and 35 ng for α9 and α10 subunits and then kept at 18 °C in ND96 buffer (96 mM NaCl, 2 mM KCl, 1 mM $CaCl_2$, 1 mM $MgCl_2$, and 5 mM HEPES, pH 7.4) supplemented with 50 mg/L gentamycin for 2−5 days before recording. Membrane currents were recorded from *Xenopus* oocytes using the two-electrode (virtual ground circuit) voltage clamp recording technique with a GeneClamp 500B amplifier (Molecular Devices, Sunnyvale, CA) and an automated workstation with eight channels in parallel, including drug delivery and online analysis (OpusXpress 6000A workstation, Axon Instruments Inc.). Both the voltage-recording and current-injecting electrodes were pulled from borosilicate glass (GC150T-15, Harvard Apparatus Ltd.) and had resistances of 0.3−1.5 MΩ when filled with 3 M KCl. All recordings were conducted at RT (21−23 °C) using a bath solution of ND96 as described above. During recordings, the oocytes were perfused continuously at a rate of 1.5 mL/min, with 300 s incubation times for the peptide. Acetylcholine (ACh; 50 μM for all nAChR subtypes) was applied for 2 s at 5 mL/min, with 360 s washout periods between applications. Cells were voltage-clamped at a holding potential of −80 mV. Data were filtered at 100 Hz and sampled at 500 Hz. Peak ACh-evoked current amplitude was measured before and following incubation of the peptide.[10] All data were pooled ($n \geq 4$ for each data point) and represent arithmetic means ± SEM. Concentration−response curves for peptide inhibition of ACh-evoked currents were fitted by unweighted nonlinear regression to the equation $E_x = E_{max}X^n/(X^n + IC_{50}{}^n)$ where E_x is the response, X is the peptide concentration, E_{max} is the maximal response, n is the slope factor, and IC_{50} the peptide concentration that gives 50% inhibition of the agonist response. Computation was done using SigmaPlot 11.0 (Systat Software, Inc., San Jose, CA).

dx.doi.org/10.1021/cb4002393 | *ACS Chem. Biol.* 2013, 8, 1815−1821

Electrophysiological Recordings of Voltage-Gated Calcium Channel Currents from Rat DRG Neurons. DRG neurons were enzymatically dissociated from 7−20 day old Wistar rats as described previously.[5] All procedures for harvesting rat DRG neurons were approved by the RMIT University Animal Ethics Committee. Whole-cell patch clamp recording was performed using a MultiClamp 700B Amplifier (Molecular Devices). Data were digitalized with a Digidata 1322A (Molecular Devices), filtered at 10 kHz, and sampled at 100 kHz using pClamp 9.2 software and MultiClamp 700B Commander (Molecular Devices). External recording solution contained (in mM) 150 TEA-Cl, 2 $BaCl_2$, 10 D-glucose, and 10 HEPES, adjusted to pH 7.4 with TEA-OH. The electrodes had a final resistance of (1−3 MΩ) with an intracellular solution containing (in mM) 140 CsCl, 1 $MgCl_2$, 5 BAPTA, and 10 HEPES adjusted to pH 7.2 with CsOH. High voltage-activated (HVA) calcium channel currents were recorded by measuring peak inward current elicited by a 150 ms depolarizing voltage step to 0 mV from a holding potential of −70 mV every 10 s. Series resistance was typically compensated at 70−80% while leak and capacitative currents were subtracted using a −P/4 pulse protocol. CGP 55845 hydrochloride was obtained from Tocris BioScience (Bristol, UK). Drugs and peptides were applied via perfusion (∼1 mL/min) in the bath solution.

■ ASSOCIATED CONTENT

Ⓢ Supporting Information

General instrumentation; peptide materials and procedures; peptide synthesis; nmr spectroscopy; modeling and simulations. This material is available free of charge via the Internet at http://pubs.acs.org.

■ AUTHOR INFORMATION

Corresponding Author

*E-mail: andrea.robinson@monash.edu.

Author Contributions

⊥These authors contributed equally to this work.

Notes

The authors declare no competing financial interest.

■ ACKNOWLEDGMENTS

The authors wish to thank the Australian Research Council for financial support of this research (LP120100414 and postgraduate scholarships to B.J.v.L., S.N.K., and S.D.R) and Dr. Brid Callaghan for preliminary studies on DRG neurons of some of the dicarba Vc1.1 analogues. D.J.A. is an ARC Australian Professorial Fellow. R.S.N. is an NHMRC Principal Research Fellow.

■ REFERENCES

(1) Sandall, D. W., Satkunanathan, N., Keays, D. A., Polidano, M. A., Liping, X., Pham, V., Down, J. G., Khalil, Z., Livett, B. G., and Gayler, K. R. (2003) A novel α-conotoxin identified by gene sequencing is active in suppressing the vascular response to selective stimulation of sensory nerves in vivo. *Biochemistry 42*, 6904−6911.

(2) Satkunanathan, N., Livett, B., Gayler, K., Sandall, D., Down, J., and Khalil, Z. (2005) Alpha-conotoxin Vc1.1 alleviates neuropathic pain and accelerates functional recovery of injured neurones. *Brain Res. 1059*, 149−158.

(3) Clark, R. J., Fischer, H., Nevin, S. T., Adams, D. J., and Craik, D. J. (2006) The synthesis, structural characterization, and receptor specificity of the α-conotoxin Vc1.1. *J. Biol. Chem. 281*, 23254−23263.

(4) Vincler, M., Wittenauer, S., Parker, R., Ellison, M., Olivera, B. M., and McIntosh, J. M. (2006) Molecular mechanism for analgesia involving specific antagonism of α9 α10 nicotinic acetylcholine receptors. *Proc. Natl. Acad. Sci. U.S.A. 103*, 17880−17884.

(5) Callaghan, B., Haythornthwaite, A., Berecki, G., Clark, R. J., Craik, D. J., and Adams, D. J. (2008) Analgesic α-conotoxins Vc1.1 and Rg1A inhibit N-type calcium channels in rat sensory neurons via $GABA_B$ receptor activation. *J. Neurosci. 28*, 10943−10951.

(6) Callaghan, B., and Adams, D. J. (2010) Analgesic α-conotoxins Vc1.1 and Rg1A inhibit N-type calcium channels in sensory neurons of α9 nicotinic receptor knockout mice. *Channels 4*, 1−4.

(7) Clark, R. J., Jensen, J., Nevin, S. T., Callaghan, B. P., Adams, D. J., and Craik, D. J. (2010) The engineering of an orally active conotoxin for the treatment of neuropathic pain. *Angew. Chem., Int. Ed. 49*, 6545−6548.

(8) Cuny, H., de Faoite, A., Huynh, T., Yasuda, T., Berecki, G., and Adams, D. J. (2012) γ-Aminobutyric acid type B ($GABA_B$) receptor expression needed for inhibition of N-type ($Ca_v2.2$) calcium channels by analgesic α-conotoxins. *J. Biol. Chem. 287*, 23948−23957.

(9) Adams, D. J., Callaghan, B., and Berecki, G. (2012) Analgesic conotoxins: Block and G protein coupled receptor modulation of N-type ($Ca_v2.2$) calcium channels. *Br. J. Pharmacol. 166*, 486−500.

(10) Nevin, S. T., Clark, R. J., Klimis, H., Christie, M. J., Craik, D. J., and Adams, D. J. (2007) Are α9 α10 nicotinic acetylcholine receptors a pain target for α-conotoxins? *Mol. Pharmacol. 72*, 1406−1410.

(11) Klimis, H., Adams, D. J., Callaghan, B., Nevin, S., Alewood, P. F., Vaughan, C. W., Mozar, C. A., and Cristie, M. J. (2011) A novel mechanism of inhibition of high-voltage activated calcium channels by α-conotoxins contributes to relief of nerve injury-induced neuropathic pain. *Pain 152*, 259−266.

(12) Livett, B. G., Sandall, D. W., Keays, D., Down, J., Gayler, K. R., Satkunanathan, N., and Khalil, Z. (2006) Therapeutic applications of conotoxins that target the neuronal nicotinic acetylcholine receptor. *Toxicon 48*, 810−829.

(13) Hossain, M. A., Rosengren, K. J., Bathgate, R. A. D., Tregear, G. W., van Lierop, B. J., Robinson, A. J., and Wade, J. D. (2009) Therapeutic applications of conotoxins that target the neuronal nicotinic acetylcholine receptor. *Org. Biomol. Chem. 7*, 1485−1736.

(14) MacRaild, C. A., Illesinghe, J., van Lierop, B. J., Townsend, A. L., Chebib, M., Livett, B. G., Robinson, A. J., and Norton, R. S. (2009) Structure and activity of (2,8)-dicarba-(3,12)-cystino α-ImI, an α-conotoxin containing a nonreducible cystine analogue. *J. Med. Chem. 52*, 755−762.

(15) Zhang, S. D., Hughes, R. A., Bathgate, R. A., Shabanpoor, F., Hossain, M. A., Lin, F., van Lierop, B. J., Robinson, A. J., and Wade, J. D. (2010) Role of the intra-A-chain disulfide bond of insulin-like peptide 3 in binding and activation of its receptor, RXFP2. *Peptides 31*, 1730−1736.

(16) Elaridi, J., Patel, J., Jackson, W. R., and Robinson, A. J. (2006) Controlled synthesis of (*S*,*S*)-2,7-diaminosuberic Acid: A method for regioselective construction of dicarba analogues of multicystine-containing peptides. *J. Org. Chem. 71*, 7538−7545.

(17) Halai, R., Clark, R. J., Nevin, S. T., Jensen, J. E., Adams, D. J., and Craik, D. J. (2009) Scanning mutagenesis of α-conotoxin Vc1.1 reveals residues crucial for activity at the α9 α10 nicotinic acetylcholine receptor. *J. Biol. Chem. 284*, 20275−20284.

(18) Celie, P. H., Kasheverov, I. E., Mordvintsev, D. Y., Hogg, R. C., van Nierop, P., van Elk, R., van Rossum-Fikkert, S. E., Zhmak, M. N., Bertrand, D., Tsetlin, V., Sixma, T. K., and Smit, A. B. (2005) Crystal structure of nicotinic acetylcholine receptor homolog AChBP in complex with an alpha-conotoxin PnIA variant. *Nat. Struct. Mol. Biol. 12*, 582−588.

(19) Wishart, D. S., Bigam, C. G., Yao, J., Abildgaard, F., Dyson, H. J., Oldfield, E., Markley, J. L., and Sykes, B. D. (1995) ^1H, ^{13}C, and ^{15}N chemical shift referencing in biomolecular NMR. *J. Biomol. NMR 6*, 135−140.

(20) Shen, Y., Delaglio, F., Cornilescu, G., and Bax, A. (2009) TALOS+: A hybrid method for predicting protein torsion angles from NMR chemical shifts. *J. Biomol. NMR 44*, 213−223.

(21) Güntert, P. (2004) Automated NMR structure calculation with CYANA. *Methods Mol. Biol. 278*, 353−378.

(22) Koradi, R., Billeter, M., and Wüthrich, K. (1996) MOLMOL: A program for display and analysis of macromolecular structures. *J. Mol. Graphics 14*, 51−55.

(23) Schwieters, C. D., Kuszewski, J. J., Tjandra, N., and Clore, G. M. (2003) The Xplor-NIH NMR molecular structure determination package. *J. Magn. Reson. 160*, 65−73.
(24) Linge, J. P., and Nilges, M. (1999) Influence of non-bonded parameters on the quality of NMR structures: a new force-field for NMR structure calculation. *J. Biomol. NMR 13*, 51−59.
(25) Laskowski, R. A., Rullmann, J. A. C., MacArthur, M. W., Kaptein, R., and Thornton, J. M. (1996) AQUA and PROCHECK-NMR: Programs for checking the quality of protein structures solved by NMR. *J. Biomol. NMR 8*, 477−496.